STNM01, the RNA oligonucleotide targeting carbohydrate sulfotransferase 15, as second-line therapy for chemotherapy-refractory patients with unresectable pancreatic cancer: An open label, phase I/IIa trial

Toshio Fujisawa,[a] Takayoshi Tsuchiya,[b] Motohiko Kato,[c] Masafumi Mizuide,[d] Kazuki Takakura,[e] Makoto Nishimura,[f] Hiromu Kutsumi,[g] Yoko Matsuda,[h] Tomio Arai,[i] Shomei Ryozawa,[d] Takao Itoi,[b] Hiroyuki Isayama,[a] Hideyuki Saya,[j] and Naohisa Yahagi[c,*]

[a]Department of Gastroenterology, Graduate School of Medicine, Juntendo University, Bunkyo-ku, Tokyo, Japan
[b]Department of Gastroenterology and Hepatology, Tokyo Medical University, Shinjuku-ku, Tokyo, Japan
[c]Division of Research and Development for Minimally Invasive Treatment, Cancer Center, Keio University School of Medicine, Shinjuku-ku, Tokyo, Japan
[d]Department of Gastroenterology, Saitama Medical University International Medical Center, Hidaka, Saitama, Japan
[e]Division of Gastroenterology and Hepatology, Department of Internal Medicine, Jikei University School of Medicine, Minato-ku, Tokyo, Japan
[f]Department of Gastroenterology, Hepatology and Nutrition, Memorial Sloan-Kettering Cancer Center, New York, NY, USA
[g]Center for Clinical Research and Advanced Medicine, Shiga University of Medical Science, Otsu, Shiga, Japan
[h]Oncology Pathology, Department of Pathology and Host-Defense, Kagawa University, Takamastu, Kagawa, Japan
[i]Department of Pathology, Tokyo Metropolitan Geriatric Hospital and Institute of Gerontology, Itabashi-ku, Tokyo, Japan
[j]Division of Gene Regulation, Institute for Advanced Medical Research, Keio University School of Medicine, Shinjuku-ku, Tokyo, Japan

eClinicalMedicine 2023;55: 101731
Published Online xxx
https://doi.org/10.1016/j.eclinm.2022.101731

Summary

Background The impact of stroma-targeting therapy on tumor immune suppression is largely unexplored. An RNA oligonucleotide, STNM01, has been shown to repress carbohydrate sulfotransferase 15 (CHST15) responsible for tumor proteoglycan synthesis and matrix remodeling. This phase I/IIa study aimed to evaluate the safety and efficacy of STNM01 in patients with unresectable pancreatic ductal adenocarcinoma (PDAC).

Methods This was an open-label, dose-escalation study of STNM01 as second-line therapy in gemcitabine plus *nab*-paclitaxel-refractory PDAC. A cycle comprised three 2-weekly endoscopic ultrasound-guided locoregional injections of STNM01 at doses of 250, 1,000, 2,500, or 10,000 nM in combination with S-1 (80–120 mg twice a day for 14 days every 3 weeks). The primary outcome was the incidence of dose-liming toxicity (DLT). The secondary outcomes included overall survival (OS), tumor response, changes in tumor microenvironment on immunohistopathology, and safety (jRCT2031190055).

Findings A total of 22 patients were enrolled, and 3 cycles were repeated at maximum; no DLT was observed. The median OS was 7.8 months. The disease control rate was 77.3%; 1 patient showed complete disappearance of visible lesions in the pancreas and tumor-draining lymph nodes. Higher tumoral CHST15 expression was associated with poor $CD3^+$ and $CD8^+$ T cell infiltration at baseline. STNM01 led to a significant reduction in CHST15, and increased tumor-infiltrating $CD3^+$ and $CD8^+$ T cells in combination with S-1 at the end of cycle 1. Higher fold increase in $CD3^+$ T cells correlated with longer OS. There were 8 grade 3 adverse events.

Interpretation Locoregional injection of STNM01 was well tolerated in patients with unresectable PDAC as combined second-line therapy. It prolonged survival by enhancing T cell infiltration in tumor microenvironment.

Abbreviations: AMED, Japan Agency for Medical Research and Development; CHST15, carbohydrate sulfotransferase 15; CI, confidence interval; CS-E, chondroitin sulfate E; CTCAE, Common Terminology Criteria for Adverse Events; DCR, disease control rate; DLT, dose-liming toxicity; ECM, extracellular matrix; EMT, epithelial mesenchymal transition; EUS-FNI, endoscopic ultrasound-guided fine needle injection; FAS, full analysis set; 5-FU, fluorouracil; GM-CSF, Granulocyte-macrophage colony-stimulating factor; IQR, interquartile range; IRB, Institutional Review Board; LV, leucovorin; MTD, maximum tolerated dose; nal-IRI, nanoliposomal irinotecan; OS, overall survival; PDAC, pancreatic ductal adenocarcinoma; PFS, progression free survival; sCD44v6, soluble CD44 variant 6; TEAE, treatment emergent adverse event; TGF, transforming growth factor

*Corresponding author. Division of Research and Development for Minimally Invasive Treatment, Cancer Center, Keio University School of Medicine, Shinjuku-ku, Tokyo, 160-8542, Japan.
E-mail address: yahagi-tky@umin.ac.jp (N. Yahagi).

Funding The present study was supported by the Japan Agency for Medical Research and Development (AMED).

Copyright © 2022 The Author(s). Published by Elsevier Ltd. This is an open access article under the CC BY-NC-ND license (http://creativecommons.org/licenses/by-nc-nd/4.0/).

Keywords: Unresectable pancreatic cancer; Carbohydrate sulfotransferase 15 (CHST15); STNM01; Tumor-infiltrating CD3+ and CD8+ T cells; Endoscopic ultrasound-guided fine needle injection

Research in context

Evidence before this study

Tumor microenvironment of pancreatic ductal adenocarcinoma (PDAC) can be characterized by desmoplastic stroma and poor infiltration of T cells, which are obstacles for anti-tumor immunotherapies. We searched PubMed for terms "pancreatic cancer/ductal adenocarcinoma", "tumor microenvironment", "clinical trial", "second line chemotherapy", "immunotherapy", "T cell", "oligonucleotide", "RNA interference", "CHST15", "proteoglycan", "stroma", "EUS" from inception up to April 2022, with no language restrictions. In this regard, only one clinical trial, "the COMBAT trial" (CXCR4 antagonist BL-8040 in combination with pembrolizumab) was shown to increase tumoral T cell infiltration with median OS of 6.6 months. Median OS of only approved *nal*-IRI +5-FU/LV regimen in second-line setting was 6.1 months.

Although the stroma represents a physical barrier for T cell infiltration, past clinical trials of anti-stromal targeted therapies did not show evidence for increased tumor-infiltrating T cells via systemic approach. Locoregional approach is currently expected to activate anti-tumor immune response and clinical trials through endoscopic ultrasound-guided fine needle injection (EUS-FNI) of oncolytic virus increases, yet T cell enhancement has not been evaluated in second-line setting.

Carbohydrate sulfotransferase 15 (CHST15) is a proteoglycan synthesizing enzyme and responsible for stromal remodeling. Silencing of local CHST15 has been shown to repress matrix remodeling in patients with Crohn's disease and animals with pulmonary and intestinal fibrosis. A small pilot trial of EUS-FNI of RNA oligonucleotide against CHST15 showed evidence of actual repression of tumoral CHST15 in patients with PDAC. However, the effect of this anti-stromal agent on tumor-infiltrating T cells in PDAC patients is unknown.

Added value of this study

EUS-guided intratumoral injection of STNM01, the RNA oligonucleotide to CHST15, showed the significant inhibition of tumoral CHST15 and led to rapid induction of tumoral T cell accumulation at week 4 as a second-line therapy in patients with unresectable PDAC. Median OS was 7.8 months. The longer OS significantly correlated with the extent of increase of tumor-infiltrating $CD3^+$ T cells at week 4. This is the first study to show that locally administered RNA oligonucleotide is able to enhance intratumoral T cell accumulation in PDAC without using immune checkpoint inhibitors or vaccinations in second-line setting.

Implications of all the available evidence

On the basis of this study, local blockade of CHST15 expression appears to be a novel immunotherapeutic option to enhance T cell infiltration in PDAC patients.

Introduction

Tumor extracellular matrix (ECM) remodeling induces tumor invasion and the development of an immunosuppressive microenvironment; both correlate with poor patient prognosis. This process is an obstacle for anti-tumor therapeutics, including immune checkpoint inhibition.[1–4] Pancreatic ductal adenocarcinoma (PDAC) is one of the most lethal tumors, and is characterized by desmoplastic stroma and poor immunogenicity.[2,5] Although first-line chemotherapy based on gemcitabine +/- *nab*-paclitaxel or FOLFIRINOX contribute to prolonged survival, most patients require second-line and further therapies. The median survival time in second-line therapy remains unfavorable, at merely 4.5 months based on historical data and 6.1 months with the currently only approved *nal*-IRI +5-FU/LV regimen[6–8]; additional treatment strategies including targeting of desmoplastic stroma or immunosuppressive pathways are therefore desired.

Tumor-derived glycans are pivotal in the modulation of ECM remodeling and the immune system during tumor progression[3,4]; however, the clinical impact of glycan-targeting therapeutics has not yet been fully investigated. Chondroitin sulfate E (CS-E) is a highly sulfated ECM glycosaminoglycan, that is solely synthesized by the Golgi enzyme carbohydrate sulfotransferase 15 (CHST15) in malignant tumor cells. CHST15 and CS-E have been reported to be highly expressed in a wide range of cancers, including progressive ovarian cancer, PDAC, brain tumors, lung,

esophageal, colorectal, and breast cancer, and osteosarcoma; they are involved in tumor cell invasion and metastasis, and correlate with poor prognosis.[9–14] The CHST15 and CS-E axes are thus potential targets for modulation of ECM remodeling and the tumor microenvironment.

STNM01 is a synthetic double-stranded RNA oligonucleotide designed to suppress CHST15 gene expression through an RNA interference mechanism.[15,16] *In vitro*, silencing of CHST15 has been found to inhibit vascular endothelial growth factor signaling, CD44-mediated invasion, and TGF-β-induced epithelial mesenchymal transition of human tumor cell lines.[10,12,14,17] *In vivo*, silencing of CHST15 leads to inhibition of tumor growth in xenograft models of nude mice and suppression of ECM remodeling in animal models.[17–21] STNM01 has been shown to downregulate CHST15 in diseased human tissues in previous clinical trials.[16,22,23] In biologics-refractory Crohn's disease and ulcerative colitis, STNM01 alleviates excessive fibrosis without complete stromal depletion, thus normalizing tissue architecture.[22–24] In an investigator-initiated pilot study on PDAC, we found that 2 of 6 patients who achieved rapid tumor CHST15 reduction showed better overall survival (OS).[16]

To overcome the hypovascular nature of PDAC, we employed the treatment approach of endoscopic ultrasound-guided fine needle injection (EUS-FNI) used in clinical settings.[16] Locoregional injection confers an advantage for RNA oligonucleotides, as the injected drug can bypass the bloodstream, be trapped by matrix fibers, be incorporated by neighboring cells.[17] Moreover, the locoregional route offers superior drug delivery to the regional lymph nodes, where the immune response can be dynamically controlled.[24,25] We aimed to better characterize the efficacy of the ECM-remodeling agent STNM01 as a second-line therapy for unresectable PDAC, taking advantage of the immune modulation observed with locoregional injections.

Methods

Study design

We conducted an open-label, dose-escalation, single arm phase I/IIa study of STNM01 as second-line therapy in gemcitabine plus nab-paclitaxel-refractory, unresectable PDAC across 5 centers in Japan (Table S1). One cycle consisted of three locoregional injections of STNM01 at 2-week intervals over 4 weeks (days 0, 14, and 28 of dosing) in combination with systemic second-line chemotherapy (Fig. S1). For phase I, a 3 + 3 dose cohort escalation design initiated with 250 nM (n = 3) followed by 1000 nM (n = 3), 2500 nM (n = 3), and 10,000 nM (n = 4) was used. Phase IIa was subsequently conducted with 9 patients in parallel with the maximum tolerated dose (MTD) or the highest dose level (10,000 nM) determined in phase I (Fig. 1). S-1 (80–120 mg) was administered orally, twice a day for 14 days with a rest period of 7 days, repeating every 3 weeks.

Participants

We enrolled patients (aged 20 years or older) who had histologically confirmed unresectable PDAC with disease progression after standard first-line chemotherapy, at least one measurable lesion, Eastern Cooperative Oncology Group Performance Status of 0 or 1, and adequate hematologic, liver, and kidney function. The investigators performed screening test after obtaining consent from the subject and confirmed that the subjects met the eligibility criteria by the screening test. The full eligibility criteria are provided in the Supplementary Appendix. All the participants provided written informed consent.

Study treatment

STNM01 dosing solutions were prepared before use at the concentrations specified (250, 1,000, 2,500, and 10,000 nM). The total dosing volume to be administered (mL) was determined based on the tumor volume (cm^3), calculated during EUS using the following formula: tumor volume (cm^3) = (minor axis [cm]^2 x major axis [cm] x 1/2) = total dosing volume (mL). The STNM01 dosing solutions were injected into the tumors with a 22G EUS fine needle following biopsy. The detailed treatment protocols are provided in the Supplementary Appendix.

Efficacy and safety evaluation

The objectives of the study were to evaluate the safety and efficacy of STNM01 as combined second-line therapy, and to determine the optimal dose level of STNM01 in patients with unresectable PDAC with progression after first-line chemotherapy. The primary outcome was the incidence of dose-limiting toxicity (DLT) at the end of cycle 1, which was determined by nonclinical monkey toxicokinetics studies. Grade 4 or higher hematologic toxicities or grade 3 or higher nonhematologic toxicities related to STNM01 were defined as DLTs. The secondary outcomes included OS, defined as the period from the day that consent was obtained as an origin time to the day of death or the day of 2 years from the consent in case of survival, tumor response assessed by the diameter of the evaluable lesions based on RECIST v1.1, immunohistopathology, safety, and pharmacokinetics. Contrast enhanced CT was performed at screening and weeks 6, 14 and 22 (Fig. S1). Progression free survival (PFS), defined as the period from the day of consent obtained to the day of first documented disease progression according to RECIST v1.1, was also assessed. For safety, adverse events were graded using the Common Terminology Criteria for Adverse Events (CTCAE) ver.5.0. For histopathology of masked biopsy

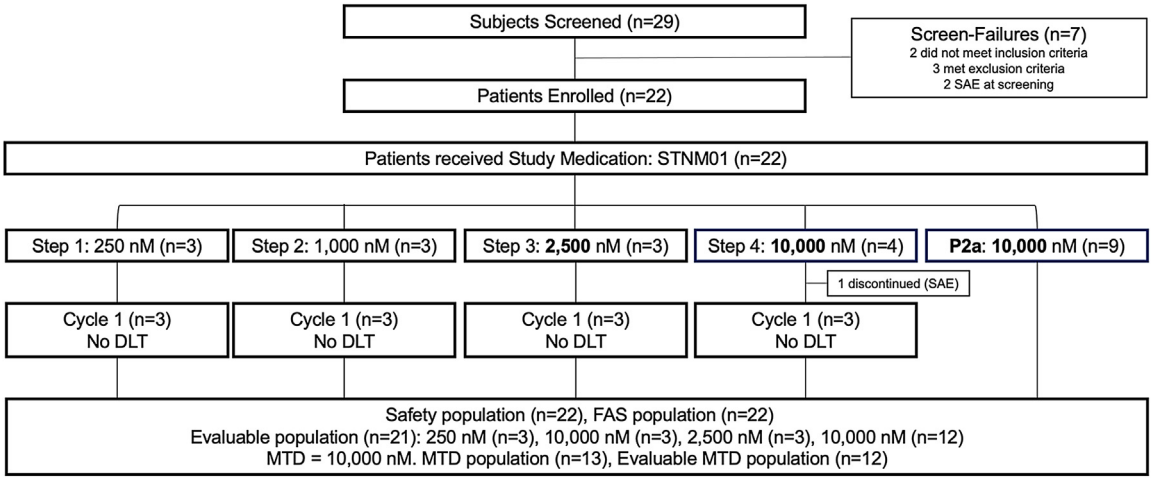

Fig. 1: **Diagram of the TME-001 trial.** enrollment and outcome of patients in the study. Reasons for screening failure and discontinuation from the study are indicated. SAE, serious adverse events; DLT, Dose limiting toxicity; MTD, Maximal Tolerated Dose.

specimens, CHST15, CD3, CD8, CD20, and CD44 variant 6 (CD44v6) positivity based on immunostaining was quantified in a blinded manner. Serum soluble CD44v6 was measured by enzyme-linked immunosorbent assay.[16] The methodology is provided in the Supplementary Appendix.

Statistical analysis

Demographic and other baseline characteristics were summarized by tabulating frequencies or providing descriptive statistics stratified for each treatment group. The number of subjects in whom TEAEs occurred and the number of events were summarized by treatment group. The safety population included all subjects who received the study drug at least once (n = 22). For continuous data, summary statistics (number of subjects, mean, standard deviation, median, IQR, and 95% confidence interval for OS, PFS, tumor diameter, serum CA19-9, serum soluble CD44v6 and positive staining for CHST15, CD3, CD8, CD20 and CD44v6 of biopsy specimens) were calculated. Statistical analysis was performed using SAS version 9.4 and GraphPad Prism version 9 with a significant level of $\alpha = 0.05$. Normality and homogeneity of variance were assessed by D'Agostino and Pearson omnibus test, Shapiro–Wilk test and F-test. For comparing continuous variables, Mann–Whitney test was used for non-Gaussian distributed data. For comparing pre- and post-values, Wilcoxon matched-pairs signed rank test was used. Exact 95% confidence intervals (2-sided) were calculated and provided where indicated. Median OS was estimated by Kaplan–Meier curves in the full analysis set (n = 22). The 95% CI for the median was calculated using Brookmeyer and Crowley method. Long-rank test was used for comparing the survival curves between FAS and MTD population. For tumor size, CHST15, CD3, CD8, CD20 and CD44v6, the percentage changes from baseline were calculated in the evaluable population (n = 21), unless otherwise indicated. The mean percentage positive areas of CHST15, CD3, CD8, CD20, or CD44v6 at baseline were compared to those at the end of cycle 1. In the exploratory analyses, the mean fold increases in the percentage positive area of CD3 or CD8 at the end of cycle 1 were compared between the patient groups who showed over 1 year survival (n = 5) and survival of 1 year or less (n = 13–14). For correlation analyses, the Pearson coefficient and the corresponding probability value (p) were calculated. All statistical tests were considered explorative, and emphasized on complete and adequate descriptive statistics.

Role of the funding source

The present study was supported by the Japan Agency for Medical Research and Development (AMED). However, AMED was not involved in any of the following: collection, analysis, and interpretation of the data, writing of the report, and the decision to submit the paper for publication. The study protocol was designed by the study coordinating committee (N.Y. and S.R.) and was approved by the Institutional Review Boards (IRBs). Data were collected by all investigators and analyzed by WDB Clinical Research Co., Ltd. All the authors interpreted the data, helped to prepare the manuscript, and made the decision to submit the manuscript for publication. All the authors declare that the study was conducted in accordance with the protocol. Each author attests to the accuracy and completeness of the reported data (registered as jRCT2031190055).

Results

Characteristics of the patients

Among 29 patients screened, 22 were enrolled and received at least 1 dose of STNM01 (Fig. 1). Demographic and baseline disease characteristics were generally balanced among the dose step groups (Table 1). All subjects (n = 22) had been treated with combined first-line gemcitabine and *nab*-paclitaxel; after progression, they received an oral fluoropyrimidine (S-1: tegafur/gimeracil/oteracil potassium combination product) as second-line therapy. Among 22 patients, 21 completed 1 cycle of treatment and were evaluable for changes from baseline; 1 discontinued due to bacteremia in the middle of cycle 1 (10,000 nM in the phase I part). The maximum administration of 3 cycles was completed in 2 patients. All patients were followed until death (maximum time observed: 22.1 months) without 2 censored patients who were followed by 24 months without death. A median follow-up time was 7.8 months (IQR: 5.9 to 18.1).

The mean percentage positive area of CHST15 was balanced, but slightly higher in the 2500 nM group (Table 1). The correlation of CHST15 expression with general and tumor microenvironmental measures at baseline were evaluated for further characterization. CHST15 did not correlate with the duration of disease and maximum tumor diameter (Fig. 2). Serum tumor markers CA19-9 (p = 0.3813, Pearson r = 0.21, 95% CI: –0.27 to 0.61) and sCD44v6 (p = 0.0158, Pearson r = 0.52, 95% CI: 0.11 to 0.78) tended to rise with increased tumoral CHST15 expression (Fig. 2). The average numbers of $CD3^+$ and $CD8^+$ T cells were 13.8 and 8.0/mm^2, respectively; both values were one tenth or less compared to those seen in resectable PDAC.[5,26] This supported the notion that in the second-line setting, PDAC patients exhibit T cell immune suppression status. CHST15 negatively correlated with CD3 (p = 0.0051, Pearson r = –0.60, 95% CI: –0.82 to –0.22) and CD8 (p = 0.0478, Pearson r = –0.45, 95% CI: –0.74 to –0.01) at baseline (Fig. 2), indicating that higher expression of CHST15 was associated with poor T cell infiltration. CD20 tended to decrease (p = –0.2402, Pearson r = –0.28, 95% CI: –0.64 to 0.19), while CD44v6 tended to increase (p = 0.0616, Pearson r = 0.41, 95% CI: –0.02 to 0.72) with higher CHST15 expression.

Safety and adverse effects

No DLT was observed, and 100 treatment emergent adverse events (TEAEs) were observed. The major TEAEs that developed in 2 or more patients are shown in Table 2. The most frequent TEAE was pyrexia (22.7%), followed by abdominal pain, hyperbilirubinemia, and decreased white blood cell count (18.2%). There were 8 grade 3 and no grade 4 TEAEs (Table S2); 17 of 100 TEAEs, all of which were of grades 1 or 2, were considered to be drug-related (27.3%) (Table S3). A total of 8 serious TEAEs were reported in 7/22 subjects (31.8%); none were drug-related (Table S4). The plasma level of STNM01 was below the detection limit at all time points after administration.

Clinical efficacy

As the MTD was not reached in phase I, phase IIa was conducted with the highest dose of 10,000 nM, and analyzed as an MTD population. The median OS was 7.8 months (95%CI: 5.9–17.0 months) in the entire

	250 nM (n = 3)	1000 nM (n = 3)	2500 nM (n = 3)	10,000 nM (n = 13)
Male (n)	1	0	1	6
Female (n)	2	3	2	7
Mean age (years) [SD]	69.7 [11.9]	66.7 [13.1]	66.3 [4.2]	65.8 [5.9]
Median duration of PDAC (months) [IQR]	14.0 [5.0–17.0]	6.0 [6.0–7.0]	6.0 [3.0–6.0]	6.0 [4.0–9.0]
Mean tumor size (mm) [SD]	47.0 [12.53]	29.4 [9.54]	34.0 [17.91]	42.4 [18.55]
Location: n (%)				
Head	0 (0.0)	2 (66.7)	0 (0.0)	3 (23.1)
Body	1 (33.3)	1 (33.3)	1 (33.3)	6 (46.2)
Tail	1 (33.3)	0 (0.0)	0 (0.0)	5 (38.5)
Other	1 (33.3)	0 (0.0)	2 (66.7)	1 (7.7)
Metastasis: n (%)	3 (100.0)	3 (100.0)	3 (100.0)	10 (76.9)
ECOG PS: n (%)				
0	3 (100.0)	3 (100.0)	2 (66.7)	12 (92.3)
1	0 (0.0)	0 (0.0)	1 (33.3)	1 (7.7)
GEM + nab-PTX as a first-line: n (%)	3 (100.0)	3 (100.0)	3 (100.0)	13 (100.0)
Combined S-1 as a second-line: n (%)	3 (100.0)	3 (100.0)	3 (100.0)	13 (100.0)
Baseline mean % positive area for CHST15 (%) [SD]	13.4 [3.9]	17.8 [8.8]	28.7 [11.1]	17.0[a] [9.4]

GEM: gemcitabine, PTX: paclitaxel, SD: Standard Deviation. [a]Mean value of the evaluable population (n = 12).

Table 1: **Demographic and baseline characteristics.**

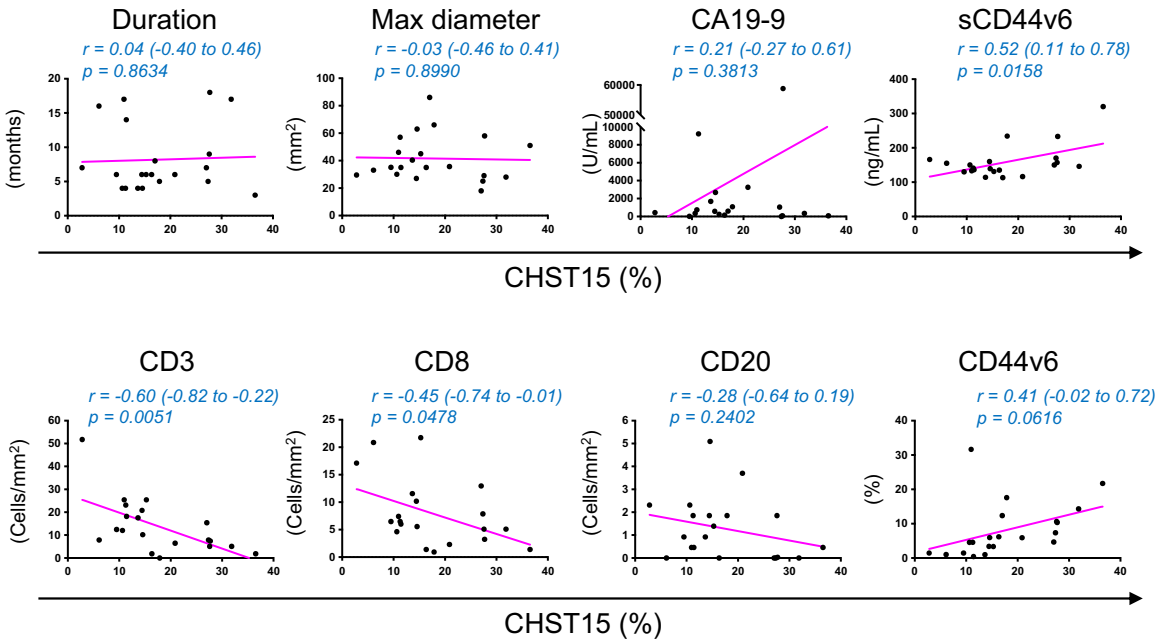

Fig. 2: **Negative correlation of baseline tumoral CHST15 with intratumoral T cells in patients with PDAC in the second-line setting.** Correlation analysis of percentage CHST15$^+$ area (x-axis) with tumor-related parameters. On the y-axis, duration of disease [Duration] (months), maximum diameter of tumor judged by enhanced CT image [Maximum diameter] (mm), serum CA19-9 (U/mL), serum sCD44v6 (ng/mL), and positive CD3$^+$, CD8$^+$, CD20$^+$, and CD44v6$^+$ expression areas (%) are shown. The related Pearson correlation coefficients with 95%CI and corresponding p values are shown.

population (n = 22) and 7.9 months (95%CI: 6.1–17.5 months) in the MTD population (n = 13) (Fig. 3a). The 6-month and 1-year survival rates of the MTD population were 84.6% and 38.4%, respectively. The median PFS was 4.3 months (95%CI: 2.0–5.3 months) in the entire population (n = 22) and 5.1 months (95%

	250 nM (n = 3)	1000 nM (n = 3)	2500 nM (n = 3)	10,000 nM (n = 13)
Overall (patients with at least one TEAE: n (%))	3 (100.0)	3 (100.0)	3 (100.0)	13 (100.0)
Cancer pain	1 (33.3)	1 (33.3)	0 (0.0)	1 (7.7)
Pancreatic carcinoma	2 (66.7)	0 (0.0)	0 (0.0)	0 (0.0)
Anemia	0 (0.0)	0 (0.0)	0 (0.0)	2 (15.4)
Decreased appetite	1 (33.3)	1 (33.3)	0 (0.0)	1 (7.7)
Hyperamylasemia	0 (0.0)	0 (0.0)	0 (0.0)	3 (23.1)
Diabetes mellitus	0 (0.0)	1 (33.3)	0 (0.0)	1 (7.7)
Hypertriglyceridemia	0 (0.0)	0 (0.0)	0 (0.0)	2 (15.4)
Hypoglycemia	0 (0.0)	0 (0.0)	0 (0.0)	2 (15.4)
Abdominal pain	2 (66.7)	1 (33.3)	0 (0.0)	1 (7.7)
Nausea	0 (0.0)	0 (0.0)	0 (0.0)	3 (23.1)
Stomatitis	1 (33.3)	0 (0.0)	0 (0.0)	2 (15.4)
Ascites	1 (33.3)	0 (0.0)	0 (0.0)	1 (7.7)
Diarrhea	0 (0.0)	0 (0.0)	0 (0.0)	1 (15.4)
Hyperbilirubinemia	0 (0.0)	0 (0.0)	0 (0.0)	4 (30.8)
Pyrexia	1 (33.3)	0 (0.0)	1 (33.3)	3 (23.1)
White blood cell count decreased	0 (0.0)	0 (0.0)	0 (0.0)	4 (30.8)
Platelet count decreased	0 (0.0)	0 (0.0)	0 (0.0)	3 (23.1)
Glycosylated hemoglobin increased	0 (0.0)	0 (0.0)	0 (0.0)	2 (15.4)
Weight decreased	0 (0.0)	1 (33.3)	0 (0.0)	1 (7.7)

MedDRA/J version (23.1).

Table 2: **Major treatment emergent adverse events (developed in 2 or more patients) during the study.**

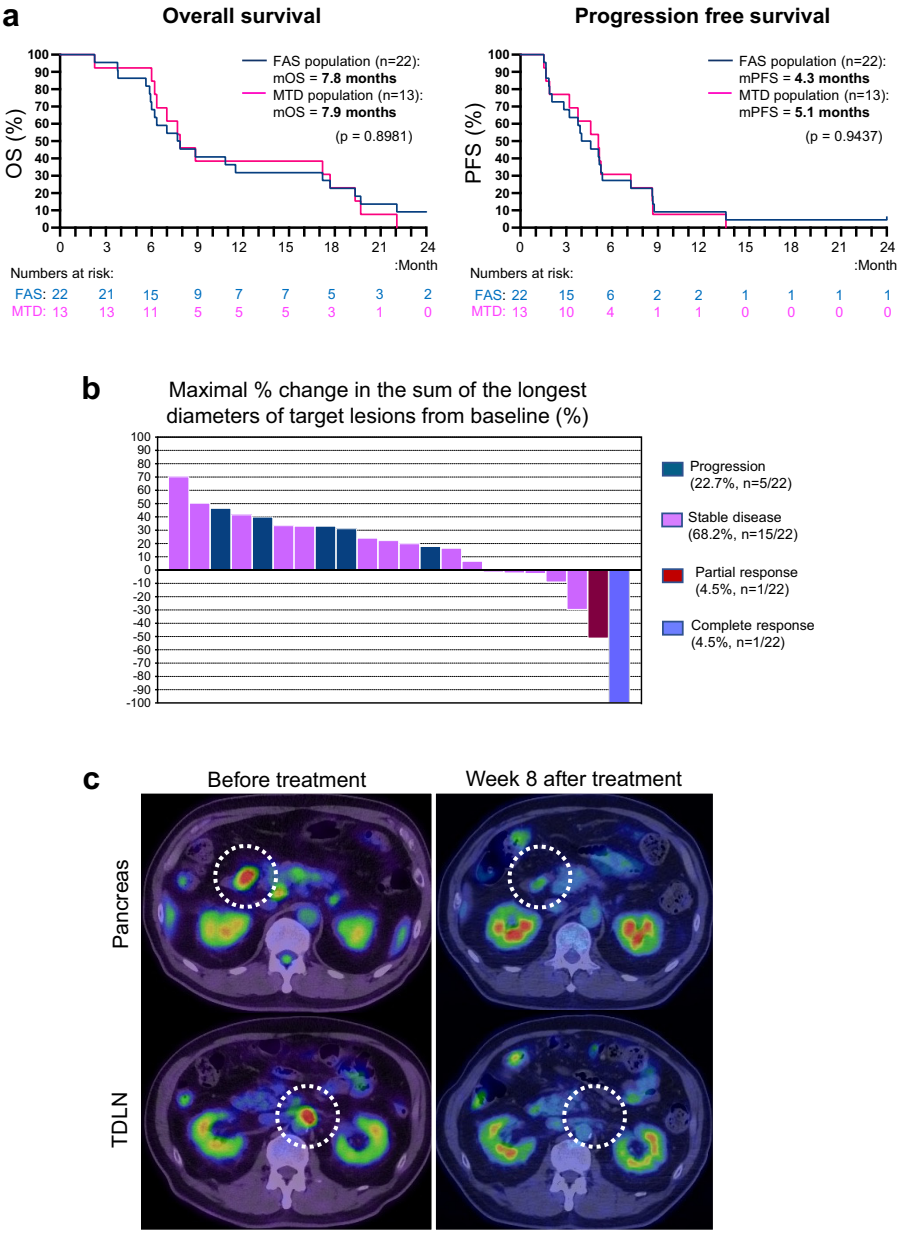

***Fig. 3*: Clinical efficacy in patients receiving STNM01 as combined second-line therapy. a.** Kaplan–Meier curves for overall survival (left) and progression free survival (right) in the entire population (n = 22, blue) and the MTD population (n = 13, magenta). P-values by Long-rank test are shown. **b.** Waterfall plot analyses for evaluable patients (n = 22), showing maximal percentage change in the sum of the longest diameters of target lesions (including local primary tumor and metastatic tumors) as compared to baseline. Blue, disease progression; purple, stable disease; maroon, partial response; orchid, complete response. **c.** PET/CT scans of a patient with complete response. Primary and metastatic paraaortic lymph node tumors are marked with dotted circles. This patient achieved complete disappearance of both tumors at the end of the first injection in cycle 2.

CI: 1.9–7.1 months) in the MTD population (n = 13) (Fig. 3a). The best overall response in the evaluable lesions included complete response (CR), partial response (PR), stable disease and progression in 1 (4.5%), 1 (4.5%), 15 (68.2%), and 5 (22.7%) patients, respectively, indicating a disease control rate of 77.3% in the FAS population (n = 22) during the observation period, that was 2 years from the consent at the maximum (Fig. 3b and Fig. S2). Notably, one patient showed complete disappearance of the visible primary and regional lymph

node metastatic tumors at the end of the first injection in cycle 2; this was at week 8 after the first treatment (Fig. 3c).

Changes in tumor microenvironmental measures

The changes in CHST15 and tumor infiltrating lymphocytes in the tumor microenvironment were evaluated by immunohistochemical staining of biopsy tissues. Abundant expression of CHST15 was mainly observed in the tumor epithelial tissue at baseline (Fig. 4a). Analysis of paired samples showed a mean reduction in percentage positive area of CHST15 from 18.02% (95%CI: 13.55 to 22.49), 16.94% (95%CI: 10.96 to 22.92) at baseline to 10.33% (95%CI: 6.5 to 14.2), 6.81% (95%CI: 2.47 to 11.62) at the end of cycle 1, in the FAS ($p < 0.0001$) and MTD ($p = 0.0005$), respectively (Fig. 4b and Fig. S3). $CD3^+$, $CD8^+$, and $CD20^+$ cells were rarely observed at baseline (Fig. 4a, Figs. S4, S5, and S6). In the MTD population, the mean percentage positive areas of CD3 and CD8 showed a 3.2- and 3.9-fold increase, respectively ($p = 0.0420$ and $p = 0.0049$, respectively; $n = 12$), at the end of cycle 1 (0.70% (95%CI: 0.33 to 1.07), 0.67% (95%CI: 0.23 to 1.11), respectively) from baseline (0.31% (95%CI: 0.20 to 0.41), 0.19% (95%CI: 0.11 to 0.26), respectively) (Fig. 4b). $CD8^+$ cells actually infiltrated the epithelial tissue of the tumor (Fig. 4a). The mean percentage positive area of CD20 showed a 16.2-fold increase (from 0.03% (95%CI: 0.02 to 0.05) at baseline to 0.24% (95%CI: −0.17 to 0.66) at the end of cycle 1), but with high variability ($p = 0.2334$, $n = 12$). In the MTD population, the mean percentage positive area of CD44v6 changed from 5.66% (95%CI: 2.96 to 8.35) at baseline to 3.89% (95%CI: 0.97 to 6.81) at the end of cycle 1 and serum sCD44v6 levels changed from 155.2 ng/mL (95%CI: 136.7 to 173.6) to 145.6 ng/mL (95%CI: 125.7 to 165.6). An example of the kinetics in a patient who received 3 cycles of treatments in phase 2a is shown in Fig. 4c. In this case, a reduction in CHST15 was seen at week 4; this was maintained thereafter. $CD3^+$ cells increased and reached a peak at week 4, while $CD8^+$ cells showed a peak at week 8 before starting cycle 2. $CD3^+$ and $CD8^+$ cells tended to decrease slightly during cycle 2, but increased again from the end of cycle 2 to within cycle 3.

Exploratory analysis

On completion of 2-year follow-up observation in all patients, we compared the parameters between the patient groups surviving over 1 year and 1 year or less. The former group showed significantly higher fold increases in CD3 (5.00 (95%CI: 1.35 to 14.53) compared to the latter: 1.02 (95%CI: 0.64 to 3.03), $p = 0.0097$) and CD8 (3.58 (95%CI: 2.67 to 9.84) compared to the latter: 1.38 (95%CI: 0.80 to 3.06, $p = 0.0183$) at week 4 (Fig. 5a). In addition, the correlation between OS and changes in T cell numbers at week 4 was analyzed in all patients. The increase in $CD3^+$ T cells at week 4 correlated significantly with longer OS ($p = 0.0039$, Pearson $r = 0.63$, 95% CI: 0.25 to 0.84, $n = 19$, Fig. 5b).

Discussion

In the present study, higher tumoral CHST15 expression was associated with poor T cell infiltration at baseline in patients with unresectable PDAC refractory to gemcitabine plus nab-paclitaxel-refractory, the first-line chemotherapy. Locoregional injection of dose-escalated STNM01 in combination with S1, the second-line chemotherapy significantly repressed tumoral CHST15. Increased $CD3^+$ and $CD8^+$ T cell infiltration was observed in the group with the highest dose (10,000 nM); the group had a median OS of 7.9 months. No serious drug-related toxicities or TEAEs of grade 3 or higher were observed; STNM01 was also not observed in the circulation in all doses.

A number of clinical trials have been conducted on stromal-depleting agents or immune checkpoint inhibitors in PDAC.[2] Although nonclinical findings indicate that depletion of stroma may improve drug delivery and lymphocyte infiltration, increased infiltration has not been demonstrated in the clinic to date. In this context, systemic hyaluronidase, a stromal-depleting agent, has not been found to improve OS when combined with standard first-line chemotherapy.[27] Scant infiltration of antitumor T cells in poorly immunogenic PDAC remains a hurdle for immune checkpoint inhibitor therapy, as most studies have failed to demonstrate an increase in T cell infiltration in microsatellite stable population. Notably, increased T cell mobilization obtained by combining a CXCR4 inhibitor and pembrolizumab confers a median OS of 6.6 months.[28] This is the longest survival in the second-line setting by immune checkpoint inhibitors, and also demonstrates the potential of tumor microenvironment modulation as an additional therapeutic approach in PDAC for the first time.

Reports suggest that CHST15 is preferentially expressed by tumor cells located at the invasive front of human PDAC tissue,[13] and is highly expressed by human tumor cell lines of the EMT phenotype.[17] However, its impact on anti-tumor T cell immunity has not been investigated. We found that tumoral CHST15 was associated with poor infiltration of $CD3^+$ and $CD8^+$ T cells in the second-line setting, and that repression of CHST15 by STNM01 rapidly and significantly increased intratumoral T cells. This suggests that CHST15 regulates T cell exclusion status in the tumor microenvironment. A direct action of STNM01 on T cells is unlikely, because CHST15 was not expressed in $CD3^+$ and $CD8^+$ T cells in the present (Fig. 4a) and previous studies.[11–14,17] STNM01 is considered to mediate indirect signals, which augment infiltration of T cells in poorly immunogenic PDACs.

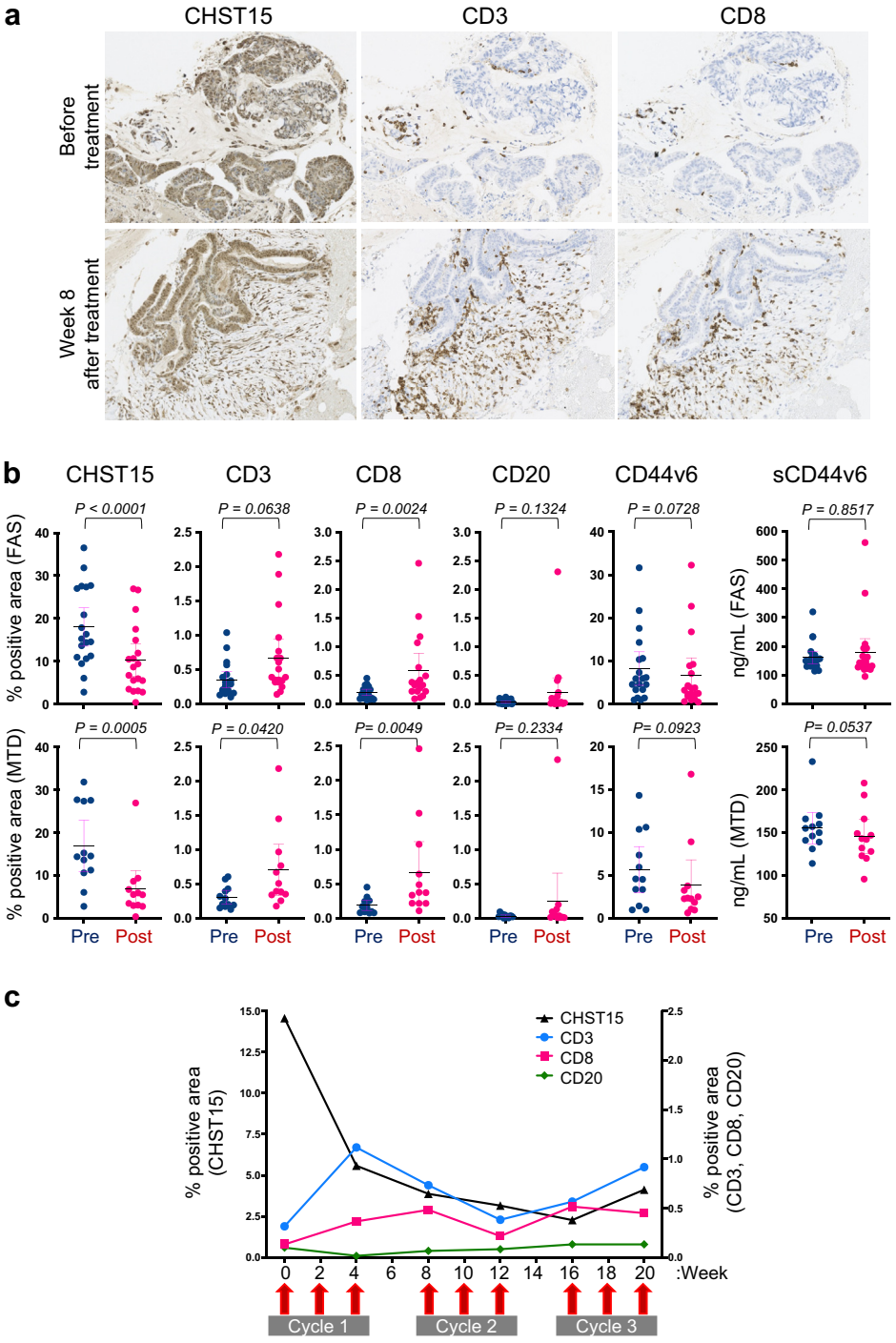

Fig. 4: **Changes in tumor microenvironmental CHST15 and lymphocytes. a.** Immunostaining for CHST15 (brown, left panels), CD3 (brown, middle panels), and CD8 (brown, right panels) in tumor specimens obtained before (upper panels) and 8 weeks after the first injection (lower panels) of STNM01. **b.** Percentage positive CHST15$^+$ (n = 19 in FAS, n = 12 in MTD), CD3$^+$ (n = 19 in FAS, n = 12 in MTD), CD8$^+$ (n = 18 in FAS, n = 12 in MTD), CD20$^+$ (n = 19 in FAS, n = 12 in MTD), and CD44v6$^+$ (n = 19 in FAS, n = 12 in MTD) areas, and serum sCD44v6 levels (n = 21 in FAS, n = 12 in MTD) at baseline (blue, W0 = week 0) and at the end of cycle 1 (magenta, W4 = week 4). Upper panels show FAS and lower panels show MTD population. Mean with 95%CI. P values determined by Wilcoxon matched-pairs signed rank test are shown. **c.** Kinetics of and positive areas for CHST15 (black line), CD3 (blue line), CD8 (magenta line), and CD20 (green line) in a patient receiving a maximum of 3 cycles of treatment with 10,000 nM STNM01.

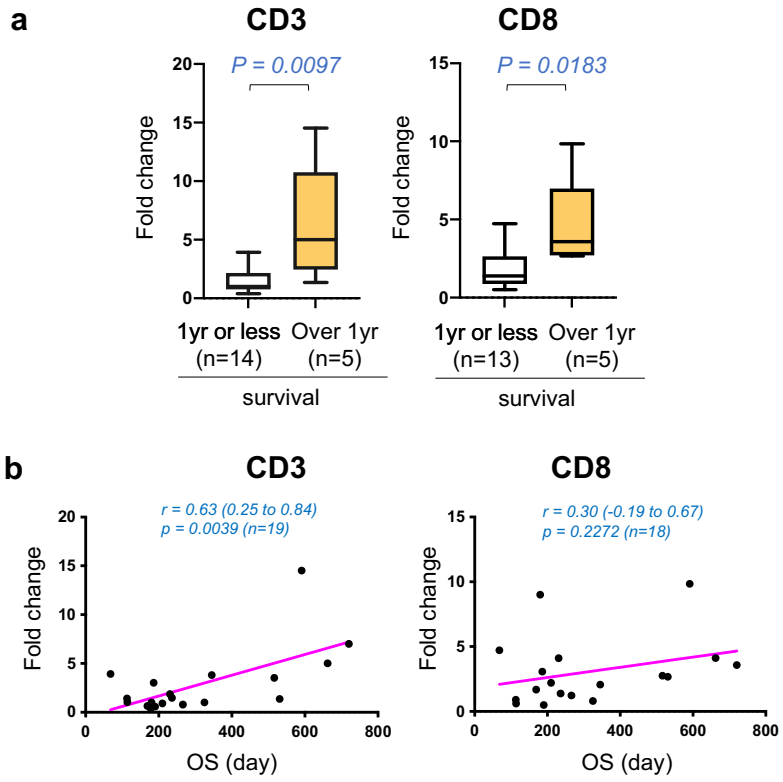

Fig. 5: **T cell infiltration at week 4 and survival. a.** Mean fold changes of the percentage positive areas of CD3 (left) and CD8 (right) at the end of cycle 1 (week 4) from baseline (week 0) are shown in the patient group with survival of 1 year (yr) or less (white boxes) and the patient group with over 1 year of survival (yellow boxes). Box and whisker plot shows median (line), 25% and 75% quartiles (box), and minimum and maximum (whiskers). No outliers defined by Turkey's method were found. The number of patients is indicated in figure. P values determined by two-tailed Mann Whitney test are shown. **b.** Correlation analysis of OS (x-axis, days) with mean fold changes (y-axis) in the percentage positive areas of CD3 (left) and CD8 (right) at the end of cycle 1 (week 4) from baseline (week 0). The related Pearson correlation coefficients with 95%CI and corresponding p values are shown.

The suppressive effect of STNM01 on tissue remodeling and fibrosis via CHST15 inhibition has been previously demonstrated in diseased tissues in both, patients[22,23] and animals.[17–21] This may be attributed to suppression of tumor stromal fibrosis by STNM01, that allow $CD3^+$ and $CD8^+$ T lymphocyte accumulation in the tumor. Fourteen out of evaluable 19 patients (73.7%) showed increased % positive area of $CD8^+$ T cells at week 4 from baseline, and finally 16 patients (84.2%) showed increased tumoral $CD8^+$ T cells from week 8 and thereafter (Fig. S5), suggesting the existence of rapid as well as delayed T cell infiltration after STNM01. Recent evidences suggest that targeting nucleotide metabolism can enhance anti-tumor immunity and its analogue therapy was shown to modulate peri-tumoral immune response in PDAC model.[24,25] In this context, enhanced T cell infiltration is considered to be induced by locoregional STNM01-mediated anti-tissue remodeling effect in combination with systemic fluoropyrimidine, although further investigation will be required to clarify the mechanism.

Regarding the median OS in the second-line setting, that reported from historical data was 4.5 months,[6] while that of S-1 monotherapy was 4.5 months in the original Japan Phase II trial and 4.9 months in the current randomized trial (MPACA-3 Trial).[28,29] The median OS of the recently approved *nal*-IRI + 5-FU/LV combination (NAPOLI-1 Trial) was 6.1 months[8]; the OS with the best immune checkpoint inhibitor combination regimen (COMBAT Trial) was 6.6 months.[30] The median OS using the present STNM01 regimen was 7.9 months in the MTD population. In this context, the 6-month survival rates in the NAPOLI-1 and COMBAT trials were 50.4% and 56.3%, respectively,[8,30] while that of the STNM01 MTD population in this study was 84.6%. Although only limited historical data are available, the 1-year survival rate of the STNM01 MTD population was 38.4%; this was higher than that observed in previous studies.[6–8,28–30] In addition, these patients showed prolonged survival for at least a further 6 months after stopping STNM01 (Fig. 3a); this pattern was not observed in the NAPOLI-1 or COMBAT trials.

The longer survival in these patients despite locoregional injection is thus considered to be due in part to rapid tumoral infiltration by T cells at only 4 weeks during cycle 1 of treatment. Patients with long-term survival over 1 year tended to achieve rapid infiltration of T cells (Fig. 5a), and the fold increase in $CD3^+$ T cells at week 4 significantly correlated with longer survival (Fig. 5b). These results suggest that rapid T cell infiltration would contribute to favorable outcomes.

The limitations of the present study included, but were not limited to, the small number of patients enrolled. Our results must be regarded as preliminary and need to be confirmed in larger clinical studies. As this was uncontrolled study, the single effect of STNM01 cannot be completely differentiated. However, we found higher DCR (77.3%) compared to historical data showing 57.5% and 37% in second-line S-1 monotherapy in Japan Phase II and MPACA-3 Trial, respectively.[28,29] Longer median PFS (4.3 months for FAS, 5.1 months for MTD) was also observed compared to 2.0 months and 2.2 months in Japan Phase II and MPACA-3 Trial, respectively. In addition, there was no grade 3 or more neutropenia, which is mediated by bone marrow suppression in fluoropyrimidine-based therapy, despite combination with S-1 in the present study. Further studies will be needed to examine if STNM01 compensates chemotherapy-induced bone marrow suppression by modulating circulating CS-E, as proteoglycans are reported to regulate the compartmentalization of GM-CSF and hematopoietic cells within bone marrow.[31] Together, we consider that STNM01 provides additional effects related to infiltration of T cells, control of tumor progression and protection from grade 3 or more neutropenia, which have not been achieved by S-1 monotherapy. Most patients showed a rapid reduction in CHST15 and increased infiltration at the end of cycle 1 (week 4); however, the optimal treatment interval needs to be defined further also from view of round feasibility of repeated EUS.

In conclusion, the data from this phase I/IIa study showed the potential of tumoral CHST15 repression by locally delivered RNA oligonucleotides in enhancing tumor infiltrating T lymphocytes and improving prognosis.

Contributors

NY, HK, SR, HS and NY contributed to the conceptualization, methods, funding acquisition, and visualization of the study. TF, TT, MK, MM, and KT contributed to the data curation, which was analyzed by TF, TT, MK, MM, KT, MN, HK, YM, TA, SR, TI, HI, HS and NY. SR, TI, HI, HS and NY contributed to data verification. TF, TT, MM, KT, SR, TI, HI, and TA contributed to the investigation and resources. NY, HK, SR, and NY contributed to the project administration. MN, SR, TI, HI, and NY supervised the study. All authors had access to all the data reported in the study and contributed to data interpretation. The first draft of the manuscript was written by TF and NY, with English editorial assistance from a medical writer. All authors reviewed and edited the manuscript and agreed to submit the manuscript for publication.

Data sharing statement

Individual participant data collected during the trials after de-identification are available for the present study. The study protocol, statistical analysis plan, and informed consent form are also available for the period between the initial three months and last five years after article publication. These requests are reviewed and approved by an independent review panel based on scientific merit. All data provided are anonymized to respect the privacy of patients who have participated in the trial, in line with applicable laws and regulations. Proposals should be directed to corresponding author at yahagi-tky@umin.ac.jp; to gain access, data requestors will need to sign a data access agreement.

Declaration of interests

Author TF received payments for lectures from Ono Pharmaceutical, Yakult Pharmaceutical Industry, Boston Scientific, Fujifilm Healthcare Corporation, Medico's Hirata, and Daiichi Sankyo. Author TT received payments for lectures from Olympus Japan, Boston Scientific Japan, and Fujifilm medical, Kaneka medix Corporation, Gadelius Medical K.K., and supports for attending meetings from Olympus Japan, Boston Scientific Japan, and Fujifilm Medical. Author MK received payments for lectures from Boston Scientific Japan, Olympus Japan, AstraZeneca, Takeda Pharmaceutical, EA Pharma, and Daiichi Sankyo, and supports for attending meetings from Olympus Japan. Author MM received payment for manuscript writing from Olympus Japan. Author MN received consulting fees from Boston Scientific, Olympus America, and Lumendi, and payment for the lecture from Takeda Pharmaceutical Company Limited. Author SR received payments for lectures from Olympus Japan, Boston Scientific Japan. Author TI received research grants from Yakult, MSD, Nippon Kayaku, AstraZeneka, Medico's Hirata Inc., Olympus Japan, Boston Scientific Japan K.K., and Gadelius Medical K.K. and consulting fees from Olympus Japan, M.I. TECH Co.,Ltd., and J-MIT K.K., and payments for lectures from Olympus Japan, Boston Scientific Japan, Gadelius Medical K.K., Asahi Kasei Pharma Corporation, Kaneka Medix Corporation, Medico's Hirata Inc., 3-D Matrix Ltd., and Takeda Pharmaceutical Company Limited. Author HI received research grants from Eisai, Ajinomoto, Yakult Honsha, Taiho Pharmaceutical, and Daiichi Sankyo, and payments for lectures from Viatris, EA Pharma, MSD, Abbie, Eizai, Otsuka Pharmaceutical, Ono Pharmaceutical, Yakult, Shionogi, Daiichi Sankyo, Taiho Pharmaceutical, Takeda Pharmaceutical, Chugai Pharmaceutical, Teijin Healthcare, AstraZeneca. Author NY received free provision of test agents from TME therapeutics, and a research grant for the present study from the Japan Agency for Medical Research and Development (AMED), research grants from Sanwa Kagaku Kenkyujo and Kaigen Pharma, and consulting fees from Olympus Japan, Top corporation, Fujifilm and Boston Scientific Japan, and payments for lectures from Olympus Japan, AstraZeneca, Daiichi Sankyo. Takeda Pharmaceuticals, Ohtsuka Pharmaceutical and EA Pharma.

Authors KT, HK, YM, TA, and HS have no declaration of interests.

Acknowledgements

We would like to thank Naoshi Yoshida, Reiko Nakamura, and Michio Wada M.D., Ph.D., of the Keio University Hospital Clinical and Translational Research Center; Miho Matsukawa M.D. of the Tokyo Metropolitan Geriatric Hospital and Institute of Gerontology; Ko Tomishima, M.D., Yusuke Takasaki, M.D., and Shigeto Ishii, M.D., Ph.D., Department of Gastroenterology, Graduate School of Medicine, Juntendo University; Ryosuke Tonozuka, M.D., Ph.D., Shuntaro Mukai, M.D., Ph.D., Takashi Kurosawa, M.D., Ph.D., and Yoshiya Yamauchi, M.D., Ph.D., Department of Gastroenterology and Hepatology, Tokyo Medical University; Yuichi Torisu, M.D., Ph.D., Division of Gastroenterology and Hepatology, Department of Internal Medicine, Jikei University School of Medicine; Shigeo Koido, M.D., Ph.D., Division of Gastroenterology and Hepatology, Department of Internal Medicine, Jikei University Kashiwa Hospital; Susumu Hijioka, M.D., Ph.D., Department of Hepatobiliary and Pancreatic Oncology, National Cancer Center Hospital; Yukiko Takayama, M.D., Ph.D. and Junichi Akao, M.D., Ph.D.,

Departments of Internal Medicine, Institute of Gastroenterology, Tokyo Women's Medical University; Shingo Ogiwara, M.D., Department of Gastroenterology, Juntendo University Urayasu Hospital; Yousuke Nakai, M.D., Ph.D. and Kei Saito, M.D., Ph.D., Department of Gastroenterology, Graduate School of Medicine, The University of Tokyo for clinical trial operations support; and Atsushi Irisawa, M.D., Ph.D., Department of Gastroenterology, Dokkyo Medical University School of Medicine and Kengo Nagashima, M.D., Ph.D., Department of Data Science, The Institute of Statistical Mathematics, Atsuhiro Masuda, M.D., Ph.D., Department of Internal Medicine, Kobe University Graduate School of Medicine for drug safety review.

Appendix A. Supplementary data

Supplementary data related to this article can be found at https://doi.org/10.1016/j.eclinm.2022.101731.

References

1 Fuster MM, Esko JD. The sweet and sour of cancer: glycans as novel therapeutic targets. *Nat Rev Cancer*. 2005;5:526–542.
2 Ho WJ, Jaffee EM, Zheng L. The tumor microenvironment in pancreatic cancer - clinical challenges and opportunities. *Nat Rev Clin Oncol*. 2020;17:527–540.
3 Mereiter S, Balmaña M, Campos D, Gomes J, Reis CA. Glycosylation in the era of cancer-targeted therapy: where are we heading? *Cancer Cell*. 2019;8:6–16.
4 Rodrigues Mantuano N, Natoli M, Zippelius A, Läubli H. Tumor-associated carbohydrates and immunomodulatory lectins as targets for cancer immunotherapy. *J Immunother Cancer*. 2020;8:e001222.
5 Orhan A, Vogelsang RP, Andersen MB, et al. The prognostic value of tumour-infiltrating lymphoc as an additional co-author by his contribution to PFS generation es in pancreatic cancer: a systematic review and meta-analysis. *Eur J Cancer*. 2020;132:71–84.
6 Nagrial AM, Chin VT, Sjoquist KM, et al. Second-line treatment in inoperable pancreatic adenocarcinoma: a systemic review and synthesis of all clinical trials. *Crit Rev Oncol-Hematol*. 2015;96:483–497.
7 Chiorean EG, Von Hoff DD, Tabernero J, et al. Second-line therapy after nab-paclitaxel plus gemcitabine or after gemcitabine for patients with metastatic pancreatic cancer. *Br J Cancer*. 2016;115:188–194.
8 Marcade TM, Chen L, Li C, et al. Liposomal Irinotecan + 5-FU/LV in metastatic pancreatic cancer. Subgroup analyses of patient, tumor, and previous treatment characteristics in the pivotal NAPOLI-1 trial. *Pancreas*. 2020;49:62–75.
9 Habuchi O, Moroi R, Ohtake S. Enzymatic synthesis of chondroitin sulfate E by N-acetylgalactosamine 4-sulfate 6-O-sulfotransferase purified from squid cartilage. *Anal Biochem*. 2002;310:129–136.
10 Mizumoto S, Yamada S, Sugahara K. Molecular interactions between chondroitin-dermatan sul2fate and growth factors/receptors/matrix proteins. *Curr Opin Struct Biol*. 2015;34:35–42.
11 tan Dam GB, van de Westerlo EMA, Purushothaman A, et al. Antibody GD3G7 selected against embryonic glycosaminoglycans defines chondroitin sulfate-E domains highly up-regulated in ovarian cancer and involved in vascular endothelial growth factor binding. *Am J Pathol*. 2007;171:1324–1333.
12 Sugahara KN, Hirata T, Tanaka T, et al. Chondroitin sulfate E fragments enhances CD44 cleavage and CD44-dependent motility in tumor cells. *Cancer Res*. 2008;68:7191–7199.
13 Matsuda Y, Fujii Y, Matsukawa M, Ishiwata T, Nishimura M, Arai T. Overexpression of carbohydrate sulfotransferase 15 in pancreatic cancer stroma is associated with worse prognosis. *Oncol Lett*. 2019;18:4100–4105.
14 Mizumoto S, Takahashi J, Sugahara K. Receptor for advanced glycation end products (RAGE) functions as receptor for specific sulfated glycosaminoglycans, and anti-RAGE antibody or sulfated glycosaminoglycans delivered in vivo inhibit pulmonary metastasis of tumor cells. *JBC*. 2012;278:18985–18994.
15 Kiryu H, Terai G, Imamura O, Yoneyama H, Suzuki K, Asai K. A detailed investigation of accessibilities around target sites of siRNAs and miRNAs. *Bioinformatics*. 2011;27:1788–1797.
16 Nishimura M, Matsukawa M, Fujii Y, et al. Effects of EUS-guided intratumoral injection of oligonucleotide STNM01 on tumor growth, histology, and overall survival in patients with unresectable pancreatic cancer. *Gastrointest Endosc*. 2018;87:1126–1131.
17 Suzuki K, Arumugam S, Yokoyama J, et al. Pivotal role of carbohydrate sulfotransferase 15 in fibrosis and mucosal healing in mouse colitis. *PLoS One*. 2016;11:e0158967.
18 Takakura K, Shibazaki Y, Yoneyama H, et al. Inhibition of cell proliferation and growth of pancreatic cancer by silencing of carbohydrate sulfotransferase 15 in vitro and in a xenograft model. *PLoS One*. 2015;10:e0142981.
19 Kai Y, Tomoda K, Yoneyama H, et al. Silencing of carbohydrate sulfotransferase 15 hinders murine pulmonary fibrosis development. *Mol Ther Nucleic Acids*. 2017;6:163–172.
20 Watanabe K, Arumugam S, Sreedhar R, et al. Small interfering RNA therapy against carbohydrate sulfotransferese 15 inhibits cardiac remodeling in rats with dilated cardiomyopathy. *Cell Signal*. 2015;27:1517–1524.
21 Sato H, Sagara S, Nakajima S, et al. Prevention of esophageal stricture after endoscopic submucosal dissection, using siRNA-based silencing of carbohydrate sulfotransferase 15 in pig. *Endoscopy*. 2017;49:491–497.
22 Suzuki K, Yokoyama J, Kawauchi Y, et al. Phase 1 clinical study of siRNA targeting carbohydrate sulfotransferase 15 in Crohn's disease patients with active mucosal lesions. *J Crohns Colitis*. 2017;11:221–228.
23 Atreya R, Kuehbacher T, Waldner M, et al. Submucosal injection of the oligonucleotide STNM01 is able to induce clinical remission, mucosal healing and histological response in left-sided ulcerative colitis patients with moderate-to-severe disease. *Gastroenterology*. 2017;152:S186.
24 Wu HL, Gong Y, Ji P, et al. Targeting nucleotide metabolism: a promising approach to enhance cancer immunotherapy. *J Hematol Oncol*. 2022;15:45.
25 Bellomo G, Rainer C, Quaranta V, et al. Chemotherapy-induced infiltration of neutrophils promotes pancreatic cancer metastasis via Gas6/AXL signalling axis. *Gut*. 2022;12. gutjnl-2021-325272.
26 Kiryu S, Ito Z, Suka M, et al. Prognostic value of immune factors in the tumor microenvironment of patients with pancreatic ductal adenocarcinoma. *BMC Cancer*. 2021;2:1197.
27 Van Cutsem E, Tempero MA, Sigal D, et al. Randomized phase III trial of pegvorhyaluronidase alfa with nab-paclitaxel plus gemcitabine for patients with hyaluronan-high metastatic pancreatic adenocarcinoma. *J Clin Oncol*. 2020;38:3185–3194.
28 Morizane C, Okusaka T, Furuse J, et al. A phase II study of S-1 in gemcitabine-refractory metastatic pancreatic cancer. *Cancer Chemother Pharmacol*. 2009;63:313–319.
29 Go SI, Lee SC, Bae WK, et al. Modified FOLFIRINOX versus S-1 as second-line chemotherapy in gemcitabine-failed metastatic pancreatic cancer patients: a randomised controlled trial (MPACA-3). *Eur J Cancer*. 2021;157:21–30.
30 Bockorny B, Macarulla T, Semenisty V, et al. Motixafortide and pembrolizumab combined to nanoliposomal irinotecan, fluorouracil, and folinic acid in metastatic pancreatic cancer: the COMBAT/KEYNOTE-202 trial. *Clin Cancer Res*. 2021;27:5020–5027.
31 Lee-Thedieck C, Schertl P, Klein G. The extracellular matrix of hematopoietic stem cell niches. *Adv Drug Deliv Rev*. 2022;181:114069.